Breakdown of Hund's rule for CuFeAs

Ze-Yi Song,[1,*] Xiu-Cai Jiang,[1,*] Xiao-Fang Ouyang,[2] and Yu-Zhong Zhang[1,†]

[1]*Shanghai Key Laboratory of Special Artificial Microstructure Materials and Technology, School of Physics Science and Engineering, Tongji University, Shanghai 200092, People's Republic of China*

[2]*School of Electronic and Electrical Engineering, Shangqiu Normal University, Shangqiu 476000, People's Republic of China*

(Received 23 September 2020; revised 7 February 2021; accepted 2 March 2021; published 11 March 2021)

The ground-state properties of CuFeAs were investigated by applying density functional theory calculations within the generalized gradient approximation (GGA) and GGA+U. We find that the bicollinear antiferromagnetic state with antiparallel orbital magnetic moments on each iron which violates the Hund's rule is favored by the on-site Coulomb interaction, which is further stabilized by Cu vacancy. The magnetic ground state can be used to understand weak antiferromagnetism in CuFeAs observed experimentally. We argue that a breakdown of the Hund's rule may be the possible origin for reduced magnetism in iron pnictides, rather than magnetic fluctuations induced by electronic correlations.

DOI: 10.1103/PhysRevB.103.125123

I. INTRODUCTION

The discovery of the high-temperature superconductivity in iron-based compounds with transition temperature T_C up to 55 K have attracted tremendous research interest for the last decade [1–4]. Similar to the phase diagram in a cuprate [5], the superconductivity in iron-based superconductors always emerge in close proximity to a state with antiferromagnetism [6–9]. Since previous theoretical studies have ruled out the phonon-mediated pairing [10], it is widely believed that the superconductivity in iron-based superconductors is unconventional and has a magnetic origin.

Therefore, much effort have been spent on revealing the origin of magnetism in iron-based superconductors. As continuous debates between the itinerant scenario [11–13] and localized picture [14,15] remain unsettled, a compromising explanation arises where the coupling of itinerant electrons and localized spins is taken into account [16,17]. In spite of the above open discussions, two consensuses have been reached. One is that density functional theory (DFT) calculations can qualitatively describe the magnetic properties of parent states in both iron pnictides and iron chalcogenides, although the magnetic moments are always overestimated due to the fact that the intermediate strength of the electronic correlations in the open d shell of an iron atom cannot be properly captured in the approximation of the functionals. The other is that in contrast to the cuprates, the effect of electronic correlations is adopted from the Hund's rule coupling [18–20], rather than on-site Coulomb repulsion. And the metallic states of iron-based superconductors are called Hund's metal, where the Hund's rule of maximum multiplicity is supposed to be valid [21].

However, the above consensuses have been seriously challenged since the discovery of CuFeAs. The magnetic susceptibility measurements showed that it is antiferromagnetic with Néel temperature T_N of around 9 K [22,23]. The antiferromagnetism was further demonstrated by neutron diffraction experiments [24,25], where either an unusual G-type antiferromagnetic order or proximity to an antiferromagnetic instability was proposed. Though ferromagnetism was also reported in the literature [26,27], it was pointed out that the weak ferromagnetism probably comes from a ferromagnetic component of a canted antiferromagnetic state [24,26]. Therefore, while the type of antiferromagnetic order is still unclear, it seems conclusive that the ground state of CuFeAs is antiferromagnetic experimentally. Nonetheless, an early theoretical study based on DFT calculations suggested that this compound is a ferromagnet [28], in stark contrast to the experimental observations [22–25], which casts doubts on the existing consensus. Obviously, further studies based on DFT calculations are required to resolve the contradiction and to clarify the magnetic structure in CuFeAs, as well as to verify the role of Hund's coupling.

Here, the nature of the magnetism of CuFeAs is investigated by applying DFT calculations. We find that the ground-state magnetic structure of CuFeAs is controlled by the As height h_{As} from the iron plane, similar to other iron-based superconductor parent compounds, and the critical height h_{c} of 1.612 Å is identified. If $h_{\mathrm{As}} < h_{\mathrm{c}}$, the ground state is in a collinear antiferromagnetic (CAFM) state. On the contrary, when As height is larger than h_c, the on-site Coulomb interaction is crucial to involve in order to correctly account for the observed antiferromagnetic state. It is found that bicollinear antiferromagnetic (BAFM) order gives the lowest total energy among the states that we studied, which becomes even more favorable in the intermediate value of on-site Coulomb interaction after introducing Cu vacancy and shows weak ferrimagnetism where the total magnetic moment turns out to be nonzero. The small magnetic moment per iron

*These authors contributed equally to this work.
†Corresponding author: yzzhang@tongji.edu.cn

is ascribed to the violation of Hund's rule [29] where antiparallel orbital magnetic moments on each iron are present. Our results can be applied to fully understand the experimental results [22–26].

CuFeAs is isostructural to 111-type iron-pnictide superconductor parent compounds LiFeAs [30] and NaFeAs [31]. It is characterized by large h_{As} in comparison to other iron pnictides, varying from $h_{\mathrm{Kam}} = 1.53$ Å [25] to $h_{\mathrm{Li}} = 1.57$ Å [23] and $h_{\mathrm{Thakur}} = 1.74$ Å [22], and, finally, to $h_{\mathrm{Zou}} = 1.80$ Å [26]. Moreover, it was reported to be nonstoichiometric [22–26], namely, the Cu vacancies are always present. Finally, like other iron-based superconductor compounds, CuFeAs is a material with large Sommerfeld coefficient, indicating that electronic interactions are not negligible [26].

II. METHOD

The DFT calculations were performed using the full-potential linearized augmented plane-wave method as implemented in the WIEN2K code [32]. We adopted the generalized gradient approximation (GGA) of Perdew-Burke-Ernzerhhor [33] for the exchange-correlation potentials. In order to determine the magnetic ground state, we have studied nonmagnetic (NM), ferromagnetic (FM), and three distinct antiferromagnetic configurations, including Néel antiferromagnetic (NAFM), CAFM, and BAFM orders [34,35]. We employed $\sqrt{2}\times\sqrt{2}\times1$ and $2\times1\times1$ unit cells for CAFM and BAFM states, and primitive cell for the other states, respectively. The Brillouin zone integration is carried out with a k mesh of $24\times24\times18$ for NM, FM, and NAFM states, and $24\times24\times20$ for the CAFM phase as well as $16\times32\times20$ for the BAFM phase, respectively. Furthermore, the influence of on-site Coulomb interaction on the magnetic stabilities of CuFeAs was investigated using the GGA+U approach [36]. The around mean-field double counting [37] is employed as CuFeAs is a correlated metal. Unless specified otherwise, the Hund's coupling $J = U/10$ [38] was used throughout all our GGA+U calculations [39]. The conclusions remain valid if J is fixed at $U/4$. Here, the experimental lattice constants reported by Thakur *et al.* [22] were used; also, the conclusions will not be altered when other experimental lattice constants are used. The x (y) of the local coordinate system for each iron is along the closest Fe-Fe bond direction.

III. RESULTS

Since it is well known that the magnetic properties of parent states of iron-based superconductors are sensitive to As height h_{As} measured from the iron plane [40,41], we first investigated the effect of h_{As} on a ground-state magnetic structure by only varying the As z positions and leaving all the other internal coordinates unchanged. Figure 1(a) shows the calculated total energies of different magnetic configurations as a function of As height within GGA. The energies of the NM state were set to zero. Starting from As height h_{Kam} of 1.53 Å, the CAFM state gives the lowest total energy. When h_{As} exceeds critical height h_c of 1.612 Å, the FM state, rather than any AFM states, becomes the stablest. The appearance of a phase transition from a CAFM state to a FM one suggests that the magnetism is strongly dependent on h_{As} in CuFeAs,

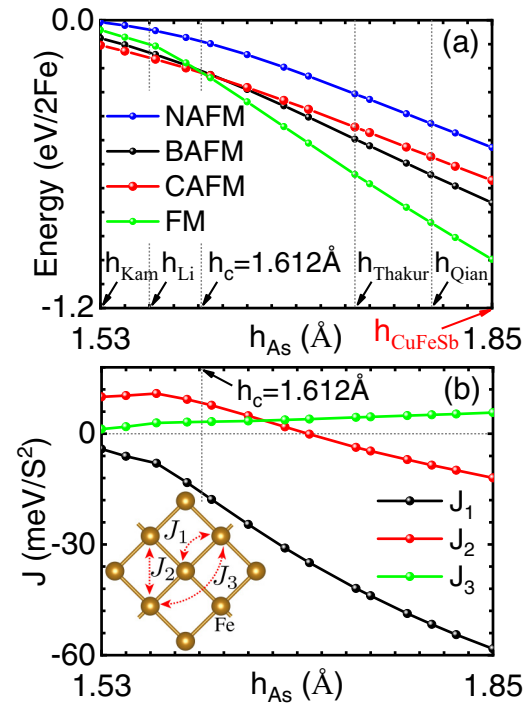

FIG. 1. (a) The calculated total energies of bicollinear antiferromagnetic (BAFM), collinear antiferromagnetic (CAFM), Néel antiferromagnetic (NAFM), ferromagnetic (FM), and nonmagnetic (NM) states as a function of As height h_{As}. Here, the energies of the NM state were set to zero. (b) By mapping the energies of ferromagnetic and various antiferromagnetic states onto a Heisenberg model, the nearest-, next-nearest-, and third-nearest-neighbor exchange couplings J_1, J_2, and J_3, respectively, were derived. The inset denotes the cartoon of the J_1, J_2, and J_3 exchange interactions.

similar to the other parent compounds of iron-based superconductors [40–42].

However, remarkable conflict can be found between the calculated results and the experimental data. As can been seen in Fig. 1(a) where various As heights reported in different experiments are shown, at h_{As} less than h_{c}, our theoretical calculations point to a CAFM ground state, which is mainly consistent with the experimental results where either long-range [23] or short-range [25] AFM order was observed, though the magnetic structure has not been determined experimentally yet. But, in the cases of h_{As} greater than h_c, while the theoretical ground state is strongly FM, it was inferred from experiments [22,24,26] that CuFeAs should be an antiferromagnet probably with ferromagnetic components. The contradiction raises a great challenge to the existing theory [34,42], which seems valid for the whole family of iron-based superconductors including both iron pnictides and iron chalcogenides, where various magnetic ground states can be correctly accounted for after different anion height is considered. In fact, the theory of anion height is also true for a sister compound of CuFeAs, so called CuFeSb, where DFT calculations [28] and experiments [43,44] both obtained a FM ground state, which can be attributed to a very high anion height of >1.84 Å. Therefore, it is urgent to understand why CuFeAs with an intermediate value of anion height is so extraordinary

that DFT calculations cannot agree with experimental findings even qualitatively.

Until now, the magnetism of iron pnictides has been explained by both the local moment picture [14,15] and the weak-coupling scenario [11–13]. From the local moment picture, the magnetic ground state can be effectively described by the frustrated Heisenberg model $H = \sum_{ij} J_{ij} S_i S_j$, where J_{ij} is the superexchange interactions between local Fe moments with spin S_i. From the above data based on the DFT calculations within GGA, the nearest-, next-nearest-, and next-next-nearest-neighbor exchange couplings J_1, J_2, and J_3 can be derived from the energy differences among various magnetic states and are summarized in Fig. 1(b). As can be seen, J_1 remains FM, and thus favors a FM order. It is strongly enhanced as a function of increased h_{As}. While J_2 is AFM and plays a dominant role at small h_{As}, it is drastically reduced in the vicinity of h_c and eventually turns into FM nature at larger h_{As}. J_3 is also AFM and barely dependent on h_{As}. If only the FM, NAFM, CAFM, and BAFM states are taken into account in the classic limit of the Heisenberg $J_1 - J_2 - J_3$ model, CAFM is energetically favorable over other magnetic configurations when $J_2 > -J_1/2$ and $J_2 > 2J_3$. The conditions are satisfied when h_{As} is smaller than h_{c}, resulting in an agreement between our first-principles results and recent experimental observations [23,25]. However, when h_{As} is greater than h_{c}, the FM state becomes the ground state owing to $J_1 < -2J_2$ and $J_1 < -J_2 - 2J_3$. Since antiferromagnetism was observed in experiments [22,24,26] when $h_{\mathrm{c}} < h_{\mathrm{As}} < 1.84$ Å, it indicates that the local moment picture fails to account for the magnetic ground state of CuFeAs in the intermediate region of anion height.

In order to know if the magnetism can be understood from the weak-coupling limit where the Fermi-surface nesting plays a role, we have calculated the orbitally resolved Pauli susceptibility $\chi^{\tau\tau}_{\tau\tau}(q)$, as defined in Refs. [45,46], to quantify the nesting property. Owing to the fact that the magnetism is mainly controlled by intraorbital particle-hole excitations, in Fig. 2 we only show the intraorbital components of the Pauli susceptibility along the path of $\Gamma - X - M - \Gamma$ in the Brillouin zone. It is found that the susceptibility of the $d_{x^2-y^2}$ and d_{z^2} orbitals is much smaller than those of the d_{xy} and $d_{yz/xz}$ orbitals, suggesting that the magnetic instabilities in CuFeAs are mainly contributed from the latter three orbitals. As is well known, a prominent peak present in the Pauli susceptibility denotes a tendency towards a certain long-range magnetic ordered state whose magnetic configuration is determined by the position of the peak in the momentum space. However, in the intermediate region of anion height, for instance, $h_{\mathrm{Thakur}} = 1.74$ Å as shown in Fig. 2(a), neither the susceptibilities of d_{xy} orbital nor those of $d_{xz/yz}$ orbitals show any pronounced peaks. On the contrary, the plateau appearing in the susceptibilities of the d_{xy} orbital along the $X - M$ path may indicate that CuFeAs is highly magnetically frustrated due to the competitions among enormous instabilities.

For comparison, we have calculated the Pauli susceptibility at low As height of 1.53 Å, as shown in Fig. 2(b). In contrast to the featureless orbital-resolved susceptibilities at $h_{\mathrm{As}} = 1.74$ Å, the counterpart at low As height shows pronounced instabilities in the d_{xy} orbital around wave vector (π, π), indicating a strong tendency towards a antiferromagnetic state. This is consistent with our total-energy calculations and previous experimental observations [23,25]. It suggests that the magnetism in CuFeAs for the $h_{\mathrm{As}} < h_c$ case can be explained by both the Fermi-surface nesting scenario [11–13] and the local moment picture [14,15], similar to all the other iron pnictides. However, if $h_c < h_{\mathrm{As}} < 1.84$ Å, neither the local moment picture nor the Fermi-surface nesting scenario could be applied to understand the magnetism in CuFeAs.

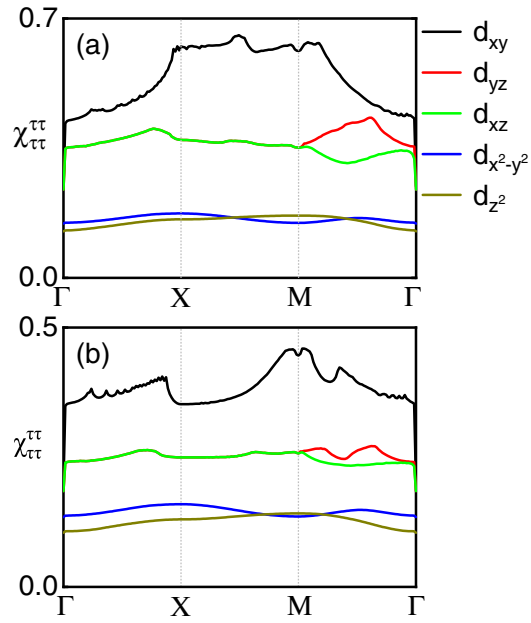

FIG. 2. The orbitally resolved Pauli susceptibilities of Fe 3*d* orbitals for As height equal to (a) 1.74 Å and (b) 1.53 Å along the high-symmetry path of $\Gamma - X - M - \Gamma$.

Considering the orbital degrees of freedom existing in CuFeAs, the inclusion of on-site Coulomb interactions may strongly change the spin and charge populations among different orbitals. Therefore, in the following, we will apply GGA+U [37] to allow for multiorbital effects and unravel the truth for a magnetic ground state in CuFeAs. Figure 3(a) shows the evolution of total energies of different magnetic configurations as a function of U. At small U, the FM state gives the lowest total energy. As U becomes large, the BAFM state becomes stabler than the other magnetic states. The FM-BAFM phase transition takes place at critical point U_c of around 4.1 eV, which is slightly smaller than the on-site Coulomb interaction $U \approx 4.5$ eV estimated from the constrained local density approximation, which is comparable to those in other iron pnictides [38]. This implies that the material is in the BAFM state and close to the phase boundary between FM and BAFM states.

Furthermore, as was observed in experiments [24,26], CuFeAs is nonstoichiometric with Cu sites being partially vacant. Cu vacancy will cause heavy hole doping and may alter the crystal-field splitting due to the deficiency of cations in certain positions. Here, the effect of Cu vacancy on the magnetic properties of the ground state was considered by simply removing one Cu from the primitive cell, leading to the chemical formula of $Cu_{0.5}FeAs$. The total energies of various

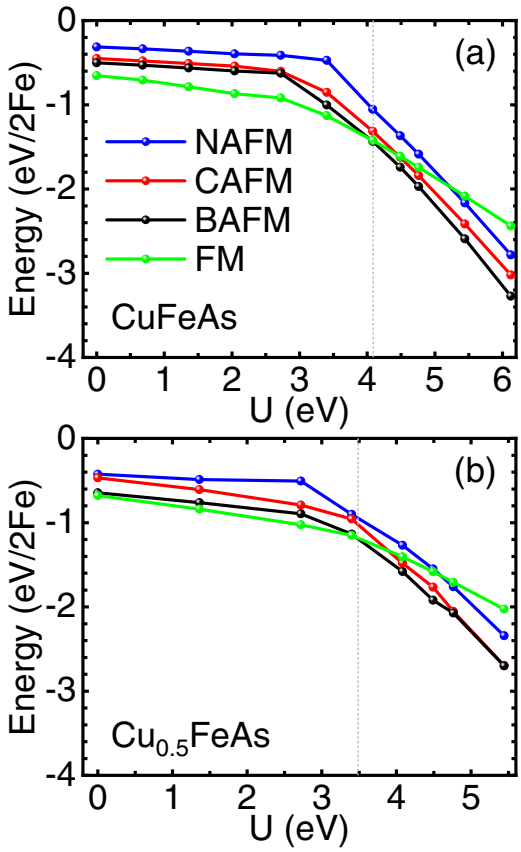

FIG. 3. The effect of on-site Coulomb interaction U on the magnetic ordering in (a) CuFeAs and (b) $Cu_{0.5}FeAs$. As U increases, the phase transition from the FM state to the BAFM state occurs (a) at around 4.1 eV for CuFeAs and (b) at about 3.5 eV for $Cu_{0.5}FeAs$, respectively.

magnetic configurations as a function of U are displayed in Fig. 3(b). Similar results are obtained as those for the stoichiometric case, except that the critical value of U is considerably suppressed from around 4.1 to about 3.5 eV, suggesting that the BAFM state is further stabilized when Cu vacancies are introduced.

To gain deep insight into the effect of on-site Coulomb interaction and Cu vacancies on the ground state, we have calculated the total and averaged magnetic moments on iron as well as orbitally resolved magnetic moments of 3d orbitals on iron for both CuFeAs and $Cu_{0.5}FeAs$. Figure 4(a) displays the averaged Fe moments. It is found that the averaged Fe moment decreases as U increases and, at critical point U_c, a sharp drop appears. The presence of Cu vacancy gives rise to a decrease of the averaged Fe moments in the FM state and an increase in the BAFM state, indicating that the Cu vacancy energetically stabilizes the BAFM state and enhances the spin polarizations in the BAFM state. In addition, if Cu vacancy is present, the total magnetic moments of Fe are finite in the BAFM state, as depicted in the inset of Fig. 4(a), which is consistent with the nonzero spontaneous magnetic moment observed in experiments [22,26].

Figures 4(b) and 4(c) show the averaged magnetic moments of Fe 3d orbitals for CuFeAs and $Cu_{0.5}FeAs$, respectively. The orbitally resolved magnetic moments are obtained by constructing atomic projectors as implemented in the WIEN2K code [32]. It is found that while the magnetic moments of the d_{xy} and $d_{yz/xz}$ orbitals which dominate the states close to the Fermi level are changed slightly in the FM state, those of d_{z^2} and $d_{x^2-y^2}$ decrease remarkably and finally become antiparallel to the magnetic moments of the d_{xy} and $d_{yz/xz}$ orbitals. Such type of breakdown of the Hund's rule was proposed to be a possible origin for the low magnetization in LaFeAsO [47–49], where DFT calculations [47] suggested that opposite magnetization among different orbitals is stabilized against the Hund's rule by the formation of large multipoles of the spin density, while model calculations based on a five-band Hubbard model [48] and a two-orbital Heisenberg model [49] found that the interorbital exchange interaction overrides the Hund's rule. From our DFT calculations and the corresponding derivations of the tight-binding model parameters using WANNIER90 [50], we conclude that both magnetic multipoles [47] and interorbital hoppings [48], which induce interorbital exchanges as the Hubbard interaction U is involved, play a role in the formation of antiparallel magnetic moments among five 3d orbitals on each iron in CuFeAs. Further increasing U, a phase transition from the FM state to a BAFM state occurs with a significant reduction

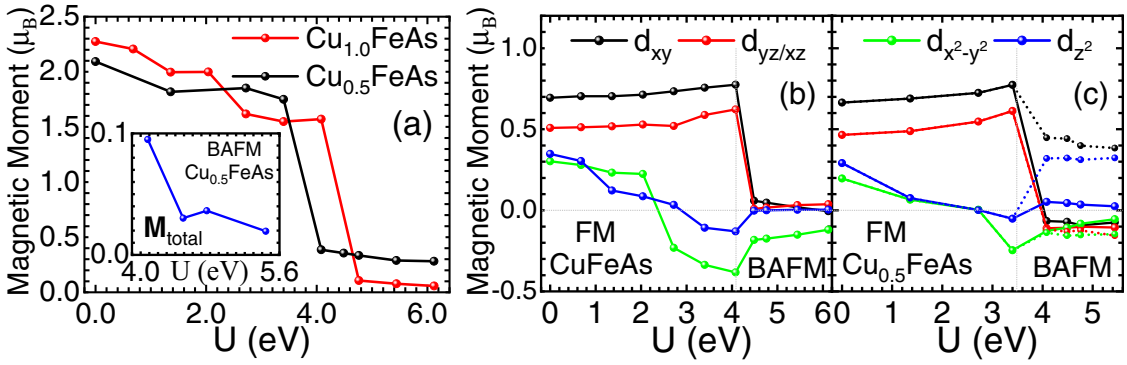

FIG. 4. (a) The averaged magnetic moment on Fe atoms for CuFeAs and $Cu_{0.5}FeAs$. The inset is the total Fe magnetic moments for $Cu_{0.5}FeAs$ in the BAFM state. The orbitally resolved magnetic moments of Fe 3d orbitals for (b) CuFeAs and (c) $Cu_{0.5}FeAs$. For $Cu_{0.5}FeAs$ in the BAFM state (c), the averaged orbital magnetic moments over the irons of the two sublattices are different, leading to the formation of a ferrimagnet.

of the magnetic moment in each orbital. However, the breakdown of the Hund's rule remains. The weak antiferromagnetism agrees well with the experimental results [22–25]. Note that in the presence of Cu vacancy, the orbital magnetic moments on different magnetic sublattices are strongly deviated from each other [Fig. 4(c)], leading to a finite total magnetic moment as shown in the inset of Fig. 4(a).

IV. DISCUSSIONS

From the above investigations, it was shown that the magnetic properties of CuFeAs vary from a CAFM state to a BAFM phase as a function of the experimental As height measured from the iron plane, where the critical height for the CAFM-BAFM transition is $h_c \approx 1.612$ Å. At the As height of $h_{As} > 1.84$ Å, the pnictogen-height driven FM phase is expected to be stablest [43,44]. This can account for various experimental observations in CuFeAs, where all magnetic susceptibility measurements at low external magnetic fields [22,23,26] suggest that this material is in an antiferromagnetic state for $1.57 \leqslant h_{As} \leqslant 1.80$ Å. At $h_{As} = 1.53$ Å, the short-range CAFM order was observed by the Mössbauer spectroscopy and muon spin resonance experiments [25], which is also qualitatively consistent with our results [shown in Fig. 1(a)] since the quantum fluctuations are completely frozen in the DFT calculations. Aware of the fact that the interlayer spin exchange hardly affects the magnetic structure in the Fe_2As_2 plane for CuFeAs, the *G*-type antiferromagnetic state, i.e., a three-dimensional NAFM state proposed in a recent study [24], cannot become the ground-state magnetic ordering because the energy of the NAFM state is higher than those of the other antiferromagnetic states that we considered, as displayed in Figs. 1(a) and 3. Besides, the agreement between our results and experiments indicates that the Coulomb interaction plays a key role in the description of the magnetism of the multiorbital system CuFeAs, especially at the intermediate As height.

Moreover, the antiferromagnetic state with nonvanishing total magnetic moments is found to be energetically stabilized when Cu vacancies are present, which explains the spontaneous magnetization in nonstoichiometric CuFeAs [22,26]. Considering the weak ferrimagnetism, CuFeAs should be susceptible to an external magnetic field. It is the reason why the magnetization exhibits the AFM-like behavior with the decrease of temperature at low magnetic fields, but shows the FM-like behavior at magnetic fields of >500 Oe due to the field-induced ferromagnetic component [22,23,26].

Finally, we found that CuFeAs is a unique compound in the family of iron pnictides that may be used to unveil the origin of weak magnetism commonly present in the pnictides. In contrast to the CAFM state at lower As height and the FM state at higher As height, both of which can be understood from the itinerant electron picture [11–13] and the localized spin scenario [14,15], the BAFM phase which can account for various experimental observations in CuFeAs [22,24,26] can only be explained by breakdown of the Hund's rule. The antiparallel arrangement of magnetic moments in different orbitals on each iron atom has been proposed as the possible origin for weak magnetism in LaFeAsO [47,48], which unfortunately was not prevalent since it was just an alternative theory to the widely accepted ones based on the itinerant or localized scenario [11–15]. However, CuFeAs may be the first counterexample which casts doubts on the applicabilities of the well-accepted theories and supports breakdown of the Hund's rule as a unified picture for the weak magnetism observed experimentally in iron pnictides. It should be noted that violation of the first Hund's rule appears in the presence of two partly filled shells such as cerium [51], while there is only one partly filled shell in CuFeAs. Moreover, Hund's coupling is always believed to dominate the correlated metallic behavior in iron pnictides [18–21], as was frequently pointed out by dynamical mean-field theory (DMFT) [52] or local density approximation (LDA)+DMFT [53] studies where nonlocal correlations are totally ignored. If breakdown of the Hund's rule was dominant, the intersite interorbital hybridizations and multipole interactions would become important, which brings the concept of Hund's metal into question and requires further investigations beyond the local approximation and Hubbard interactions. Also, breakdown of the Hund's rule may provide a new route to form singlet Cooper pairs locally [54].

Note that the CuFeAs is unique among iron pnictides due to the fact that it possesses the highest arsenic height in comparison to other iron arsenic compounds, for example, $h_{As} \sim 1.51$ Å for LiFeAs [55], 1.31 Å for LaFeAsO [6], and 1.35 Å for $BaFe_2As_2$ [56]. And it is even higher than that of $Fe_{1.01}Se$, where $h_{Se} \sim 1.47$ Å [57]. The height is comparable to $h_{Te} \sim 1.75$ Å of $Fe_{1.068}Te$, which also shows bicollinear antiferromagnetic order [58]. However, it is smaller than $h_{Sb} \sim 1.84$ Å of CuFeSb, where ferromagnetism is observed [43,44].

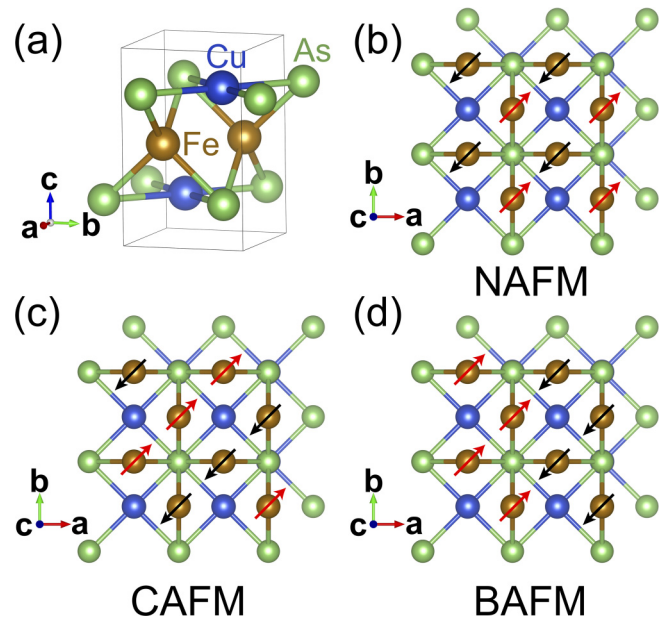

FIG. 5. (a) Crystal structure of CuFeAs used in this work, where the blue, brown, and green atoms denote Cu, Fe, and As, respectively. The top-view cartoons for the (b) Néel antiferromagnetic state (NAFM), (c) collinear antiferromagnetic state (CAFM), and (d) bicollinear antiferromagnetic state (BAFM), where the red and black arrows represent two different spin species on Fe atoms which form a square lattice.

V. CONCLUSION

In conclusion, we have investigated the magnetism of CuFeAs by applying DFT calculations. It is found that breakdown of Hund's rule occurs and is responsible for the exotic BAFM state in CuFeAs at the height of the As atom of $1.612 < h_{\mathrm{As}} < 1.84$ Å. This phase intersects between a CAFM state at $h < 1.612$ Å and a FM state at $h > 1.84$ Å. The presence of Cu vacancy favors the BAFM state and induces weak ferrimagnetism due to the symmetry breaking between the magnetic sublattices. The interaction is indispensable to correctly capture the ground state of CuFeAs. Our results can be applied to fully understand experimental observations and have an important implication that breakdown of the Hund's rule may be a unified theory for weak magnetism in iron pnictides.

ACKNOWLEDGMENTS

This work is financially supported by the National Natural Science Foundation of China (Grants No. 11774258 and No. 12004283) and the Postgraduate Education Reform Project of Tongji University (Grant No. GH1905). Z.Y.S. acknowledges the financial support by the China Postdoctoral Science Foundation (Grant No. 2019M651563).

APPENDIX: CRYSTAL STRUCTURE OF CuFeAs AND ANTIFERROMAGNETIC STRUCTURES STUDIED IN THE WORK

Figure 5 shows the crystal structure of CuFeAs and antiferromagnetic structures studied in this work.

[1] Y. Kamihara, T. Watanabe, M. Hirano, and H. Hosono, Iron-based layered superconductor $LaO_{1-x}F_xFeAs$ ($x = 0.05$–0.12) with $T_c = 26$ K, J. Am. Chem. Soc. **130**, 3296 (2008).

[2] M. Rotter, M. Tegel, and D. Johrendt, Superconductivity at 38 K in the Iron Arsenide $(Ba_{1-x}K_x)Fe_2As_2$, Phys. Rev. Lett. **101**, 107006 (2008).

[3] R. Zhi-An, L. Wei, Y. Jie, Y. Wei, S. Xiao-Li, L. Zheng-Cai, C. Guang-Can, D. Xiao-Li, S. Li-Ling, Z. Fang, and Z. Zhong-Xian, Superconductivity at 55 K in iron-based F-doped layered quaternary compound $Sm[O_{1-x}F_x]FeAs$, Chin. Phys. Lett. **25**, 2215 (2008).

[4] G. R. Stewart, Superconductivity in iron compounds, Rev. Mod. Phys. **83**, 1589 (2011).

[5] B. Keimer, S. A. Kivelson, M. R. Norman, S. Uchida, and J. Zaanen, From quantum matter to high-temperature superconductivity in copper oxides, Nature (London) **518**, 179 (2015).

[6] C. de la Cruz, Q. Huang, J. W. Lynn, J. Li, W. Ratcliff, II, J. L. Zarestky, H. A. Mook, G. F. Chen, J. L. Luo, N. L. Wang, and P. Dai, Magnetic order close to superconductivity in the iron-based layered $LaO_{1-x}F_xFeAs$ systems, Nature (London) **453**, 899 (2008).

[7] D. N. Basov and A. V. Chubukov, Manifesto for a higher T_c, Nat. Phys. **7**, 272 (2011).

[8] D. J. Scalapino, A common thread: The pairing interaction for unconventional superconductors, Rev. Mod. Phys. **84**, 1383 (2012).

[9] L. de' Medici, G. Giovannetti, and M. Capone, Selective Mott Physics as a Key to Iron Superconductors, Phys. Rev. Lett. **112**, 177001 (2014).

[10] L. Boeri, O. V. Dolgov, and A. A. Golubov, Is $LaFeAsO_{1-x}F_x$ an Electron-Phonon Superconductor?, Phys. Rev. Lett. **101**, 026403 (2008).

[11] I. I. Mazin, D. J. Singh, M. D. Johannes, and M. H. Du, Unconventional Superconductivity with a Sign Reversal in the Order Parameter of $LaFeAsO_{1-x}F_x$, Phys. Rev. Lett. **101**, 057003 (2008).

[12] J. Dong, H. J. Zhang, G. Xu, Z. Li, G. Li, W. Z. Hu, D. Wu, G. F. Chen, X. Dai, J. L. Luo, Z. Fang, and N. L. Wang, Competing orders and spin-density-wave instability in $La(O_{1-x}F_x)FeAs$, Europhys. Lett. **83**, 27006 (2008).

[13] I. I. Mazin, Superconductivity gets an iron boost, Nature (London) **464**, 183 (2010).

[14] T. Yildirim, Origin of the 150-K Anomaly in LaFeAsO: Competing Antiferromagnetic Interactions, Frustration, and a Structural Phase Transition, Phys. Rev. Lett. **101**, 057010 (2008).

[15] Q. Si and E. Abrahams, Strong Correlations and Magnetic Frustration in the High T_c Iron Pnictides, Phys. Rev. Lett. **101**, 076401 (2008).

[16] M. D. Johannes and I. I. Mazin, Microscopic origin of magnetism and magnetic interactions in ferropnictides, Phys. Rev. B **79**, 220510(R) (2009).

[17] Yi-Zhuang You, F. Yang, Su-Peng Kou, and Zheng-Yu Weng, Magnetic and superconducting instabilities in a hybrid model of itinerant/localized electrons for iron pnictides, Phys. Rev. B **84**, 054527 (2011).

[18] K. Haule and G. Kotliar, Coherence-incoherence crossover in the normal state of iron oxypnictides and importance of Hund's rule coupling, New J. Phys. **11**, 025021 (2009).

[19] Z. P. Yin, K. Haule, and G. Kotliar, Magnetism and charge dynamics in iron pnictides, Nat. Phys. **7**, 294 (2011).

[20] N. Lanatà, H. U. R. Strand, G. Giovannetti, B. Hellsing, L. de' Medici, and M. Capone, Orbital selectivity in Hund's metals: The iron chalcogenides, Phys. Rev. B **87**, 045122 (2013).

[21] A. Georges, L. de' Medici, and J. Mravlje, Strong correlations from Hund's coupling, Annu. Rev. Condens. Matter Phys. **4**, 137 (2013).

[22] G. S. Thakur, Z. Haque, L. C. Gupta, and A. K. Ganguli, CuFeAs: A new member in the 111-family of iron-pnictides, J. Phys. Soc. Jpn. **83**, 054706 (2014).

[23] K. Li, D. Yuan, J. Guo, and X. Chen, Observation of direct evolution from antiferromagnetism to superconductivity in $Cu_{1-x}Li_xFeAs$ ($0 \leqslant x \leqslant 1.0$), Phys. Rev. B **97**, 134503 (2018).

[24] T. Zou, C. C. Lee, W. Tian, H. B. Cao, M. Zhu, B. Qian, C. R. dela Cruz, W. Ku, Z. Q. Mao, and X. Ke, *G*-type magnetic order in ferropnictide $Cu_xFe_{1-y}As$ induced by hole doping on As sites, Phys. Rev. B **95**, 054414 (2017).

[25] S. Kamusella, Hans-Henning Klauss, G. S. Thakur, Z. Haque, L. C. Gupta, A. K. Ganguli, I. Kraft, U. Burkhardt, H. Rosner, H. Luetkens, J. W. Lynn, and Y. Zhao, Magnetism and site exchange in CuFeAs and CuFeSb: A microscopic and theoretical investigation, Phys. Rev. B **95**, 094415 (2017).

[26] B. Qian, J. Hu, J. Liu, Z. Han, P. Zhang, L. Guo, X. Jiang, T. Zou, M. Zhu, C. R. Dela Cruz, X. Ke, and Z. Q. Mao,

Weak ferromagnetism of $Cu_xFe_{1+y}As$ and its evolution with Co doping, Phys. Rev. B **91**, 014504 (2015).
[27] B. Lv, Ph.D. thesis, University of Houston, 2009.
[28] G. Wang, X. Shi, and D. Wang, Pnictide-height dependent ferromagnetism in CuFeAs and CuFeSb, J. Alloys Compd. **686**, 38 (2016).
[29] Due to the presence of a tetragonal crystal field in iron-based compounds, together with the negligible strength of spin-orbit coupling in iron, the orbital angular momentum of 3*d* orbitals is completely quenched in CuFeAs. Therefore, the second and the third Hund's rules are irrelevant in CuFeAs and, throughout the paper, the Hund's rule refers to the first one.
[30] J. H. Tapp, Z. Tang, B. Lv, K. Sasmal, B. Lorenz, P. C. W. Chu, and A. M. Guloy, LiFeAs: An intrinsic FeAs-based superconductor with $T_c = 18$ K, Phys. Rev. B **78**, 060505(R) (2008).
[31] S. Li, C. de la Cruz, Q. Huang, G. F. Chen, T.-L. Xia, J. L. Luo, N. L. Wang, and P. Dai, Structural and magnetic phase transitions in $Na_{1-\delta}FeAs$, Phys. Rev. B **80**, 020504(R) (2009).
[32] K. Schwarz, P. Blaha, and G. K. H. Madsen, Electronic structure calculations of solids using the WEIN2K package for material sciences, Comput. Phys. Commun. **147**, 71 (2002).
[33] J. P. Perdew, K. Burke, and M. Ernzerhof, Generalized Gradient Approximation Made Simple, Phys. Rev. Lett. **77**, 3865 (1996).
[34] Wei-Guo Yin, Chi-Cheng Lee, and W. Ku, Unified Picture for Magnetic Correlations in Iron-Based Superconductors, Phys. Rev. Lett. **105**, 107004 (2010).
[35] See also cartoons for these magnetic states in the appendix.
[36] A. I. Liechtenstein, V. I. Anisimov, and J. Zaanen, Density-functional theory and strong interactions: Orbital ordering in Mott-Hubbard insulators, Phys. Rev. B **52**, R5467 (1995).
[37] M. T. Czyżyk and G. A. Sawatzky, Local-density functional and on-site correlations: The electronic structure of La_2CuO_4 and $LaCuO_3$, Phys. Rev. B **49**, 14211 (1994).
[38] T. Miyake, K. Nakamura, R. Arita, and M. Imada, Comparison of *Ab initio* low-energy models for LaFePO, LaFeAsO, $BaFe_2As_2$, LiFeAs, FeSe, and FeTe: Electron correlation and covalency, J. Phys. Soc. Jpn. **79**, 044705 (2010).
[39] The explicit inclusion of on-site Coulomb repulsion U and exchange parameter J which favors the first Hund's rule and thus is so-called the Hund's coupling term allows us to investigate multi-orbital physics in CuFeAs. In contrast to the conventional understanding where maximum multiplicity should appear in the presence of the Hund's coupling, breakdown of the Hunds rule occurs in CuFeAs, resulting in an exotic BAFM state with small magnetic moment.
[40] T. Yildirim, Strong Coupling of the Fe-Spin State and the As-As Hybridization in Iron-Pnictide Superconductors from First-Principle Calculations, Phys. Rev. Lett. **102**, 037003 (2009).
[41] Z. P. Yin, S. Lebègue, M. J. Han, B. P. Neal, S. Y. Savrasov, and W. E. Pickett, Electron-Hole Symmetry and Magnetic Coupling in Antiferromagnetic LaFeAsO, Phys. Rev. Lett. **101**, 047001 (2008).
[42] Chang-Youn Moon and Hyoung Joon Choi, Chalcogen-Height Dependent Magnetic Interactions and Magnetic Order Switching in $FeSe_xTe_{1-x}$, Phys. Rev. Lett. **104**, 057003 (2010).
[43] B. Qian, J. Lee, J. Hu, G. C. Wang, P. Kumar, M. H. Fang, T. J. Liu, D. Fobes, H. Pham, L. Spinu, X. S. Wu, M. Green, S. H. Lee, and Z. Q. Mao, Ferromagnetism in CuFeSb: Evidence of competing magnetic interactions in iron-based superconductors, Phys. Rev. B **85**, 144427 (2012).
[44] A. Sirohi, C. K. Singh, G. S. Thakur, P. Saha, S. Gayen, A. Gaurav, S. Jyotsna, Z. Haque, L. C. Gupta, M. Kabir, A. K. Ganguli, and G. Sheet, High spin polarization and the origin of unique ferromagnetic ground state in CuFeSb, Appl. Phys. Lett. **108**, 242411 (2016).
[45] S. Graser, T. A. Maier, P. J. Hirschfeld, and D. J. Scalapino, Near-degeneracy of several pairing channels in multiorbital models for the Fe pnictides, New J. Phys. **11**, 025016 (2009).
[46] Ming-Cui Ding, Hai-Qing Lin, and Yu-Zhong Zhang, Hidden $(\pi, 0)$ instability as an itinerant origin of bicollinear antiferromagnetism in $Fe_{1+x}Te$, Phys. Rev. B **87**, 125129 (2013).
[47] F. Cricchio, O. Grånäs, and L. Nordström, Low spin moment due to hidden multipole order from spin-orbital ordering in LaFeAsO, Phys. Rev. B **81**, 140403(R) (2010).
[48] E. Bascones, M. J. Calderón, and B. Valenzuela, Low Magnetization and Anisotropy in the Antiferromagnetic State of Undoped Iron Pnictides, Phys. Rev. Lett. **104**, 227201 (2010).
[49] C. Liu, Dao-Xin Yao, and A. W. Sandvik, Two-orbital quantum spin model of magnetism in the iron pnictides, Phys. Rev. B **85**, 094410 (2012).
[50] A. A. Mostofi, J. R. Yates, Young-Su Lee, I. Souza, D. Vanderbilt, and N. Marzari, WANNIER90: A tool for obtaining maximally-localised Wannier functions, Comput. Phys. Commun. **178**, 685 (2008).
[51] J. D. Morgan and W. Kutzelnigg, Hund's rules, the alternating rule, and symmetry holes, J. Phys. Chem. **97**, 2425 (1993).
[52] A. Georges, G. Kotliar, W. Krauth, and M. J. Rozenberg, Dynamical mean-field theory of strongly correlated fermion systems and the limit of infinite dimensions, Rev. Mod. Phys. **68**, 13 (1996).
[53] G. Kotliar, S. Y. Savrasov, K. Haule, V. S. Oudovenko, O. Parcollet, and C. A. Marianetti, Electronic structure calculations with dynamical mean-field theory, Rev. Mod. Phys. **78**, 865 (2006).
[54] S. Hoshino and P. Werner, Spontaneous Orbital-Selective Mott Transitions and the Jahn-Teller Metal of A_3C_{60}, Phys. Rev. Lett. **118**, 177002 (2017).
[55] M. J. Pitcher, D. R. Parker, P. Adamson, S. J. C. Herkelrath, A. T. Boothroyd, R. M. Ibberson, M. Brunelli, and S. J. Clarke, Structure and superconductivity of LiFeAs, Chem. Commun. **45**, 5918 (2008).
[56] Q. Huang, Y. Qiu, W. Bao, M. A. Green, J. W. Lynn, Y. C. Gasparovic, T. Wu, G. Wu, and X. H. Chen, Neutron-Diffraction Measurements of Magnetic Order and a Structural Transition in the Parent $BaFe_2As_2$ Compound of FeAs-Based High-Temperature Superconductors, Phys. Rev. Lett. **101**, 257003 (2008).
[57] T. M. McQueen, Q. Huang, V. Ksenofontov, C. Felser, Q. Xu, H. Zandbergen, Y. S. Hor, J. Allred, A. J. Williams, D. Qu, J. Checkelsky, N. P. Ong, and R. J. Cava, Extreme sensitivity of superconductivity to stoichiometry in $Fe_{1+\delta}Se$, Phys. Rev. B **79**, 014522 (2009).
[58] S. Li, C. de la Cruz, Q. Huang, Y. Chen, J. W. Lynn, J. Hu, Y.-L. Huang, F.-C. Hsu, K.-W. Yeh, M.-K. Wu, and P. Dai, First-order magnetic and structural phase transitions in $Fe_{1+y}Se_xTe_{1-x}$, Phys. Rev. B **79**, 054503 (2009).